CERN
CH-1211 Geneva 23
Switzerland

LHC

EDMS NO.	REV.	VALIDITY
1995306	**0.4**	**DRAFT**

REFERENCE
LHC-LBH-EC-0001

Date: 2019-02-01

ENGINEERING CHANGE REQUEST

Installation of the 11 T Dipole Full Assembly in LHC P7 (HL-LHC WP11)

BRIEF DESCRIPTION OF THE PROPOSED CHANGE(S):

It is foreseen to substitute in the DS region at point 7 two 14.3 m long 8.33 T standard LHC main dipoles (MB) each with a cryo-assembly composed by a pair of 5.5 m-long 11 T dipoles with in the middle a 3.3 m long bypass cryostat, in which is hosted a TCLD collimator. Thanks to this change the design losses can be sustained without quench.

DOCUMENT PREPARED BY:	DOCUMENT TO BE CHECKED BY:	DOCUMENT TO BE APPROVED:
D. Schoerling et al.	**HiLumi-WP11-Integration** C. Adorisio, G. Arduini, V. Baglin, M. Barberan, I. Bejar Alonso, N. Bellegarde, M. Bernardini, C. Bertone, C. Boccard, L. Bottura, G. Bregliozzi, M. Brugger, J.P. Burnet, S. Bustamante, S. Chemli, F. Cerutti, P. Chiggiato, J. P. Corso, D. Delikaris, B. Delille, R. Denz, A. Devred, R. de Maria, S. Evrard, P. Fessia, R. Folch, A. Foussat, J.- F. Fuchs, C. Gaignant, M. Giovannozzi, G. Girardot, J.-L. Grenard, M. Lamont, S. Le Naour, M. Martino, D. Missiaen, M. Modena, V. Montabonnet, Y. Muttoni, M. Nonis, T. Otto, E. Page, S. Redaelli, D. Ricci, I. Romera Ramirez, B. Salvant, F. Savary, J. Sestak, A. Siemko, R. Steerenberg, L. Tavian, M. Tavlet, C. Vollinger, J. Wenninger, M. Zerlauth, A. Lechner, C. Bahamonde Castro, C. Zamantos.	P. Collier (on behalf of LMC) L. Rossi (on behalf of the HL-LHC project)

DOCUMENT SENT FOR INFORMATION TO:

ATS Group Leaders

SUMMARY OF THE ACTIONS TO BE UNDERTAKEN:

Following drawings and documents need to be updated, once the change is being performed:
-Survey reference drawings to be created (D. Missiaen)
-LHCLSD7_0002, LHCLSD7_0004, LHCEY___7001, and LHCEY___7008 (P. Orlandi (responsible) and M. Zerlauth)
-LHCLSQR_0032 and LHCLSQR_0033 (R. van Weelderen)
-LHCLSVI_0020 and LHCLSVI_0031 (P. Cruikshank)
-LHCQQ_IG0033 and LHC-LI-ES-0017 (JP. Tock)
-LHC-LBA-ES-0011, LHC-LI-ES-0001, LHC-LE-ES-0001, and LHC-LE-ES-0002 (D. Duarte)
-LHCLSSH_0013 and LHCLSSH_0014 (M. Amparo Gonzalez De La Aleja Cabana)
-LHCLJ_7U0085 (C9.L7) and LHCLJ_7U0087 (C9.R7) (J. Oliveira)

Note: When approved, an Engineering Change Request becomes an Engineering Change Order.

1. INTRODUCTION

This ECR describes all necessary actions and required changes for the substitution of two 14.3 m long 8.33 T standard LHC main dipoles (MB) each with an assembly consisting out of a pair of 5.5 m-long 11 T dipoles surrounding the bypass cryostat and the Target Collimator Long Dispersion suppressor (TCLD) [1], where the latter is treated in a separate ECR by WP5 (HL Collimation) [2].

The present state of the areas concerned is shown in Figures 1 and 2.

Figure 1 — Picture of area under change, cell 9.L7 at R72 – present MB.B8L7 (18/02/2019)

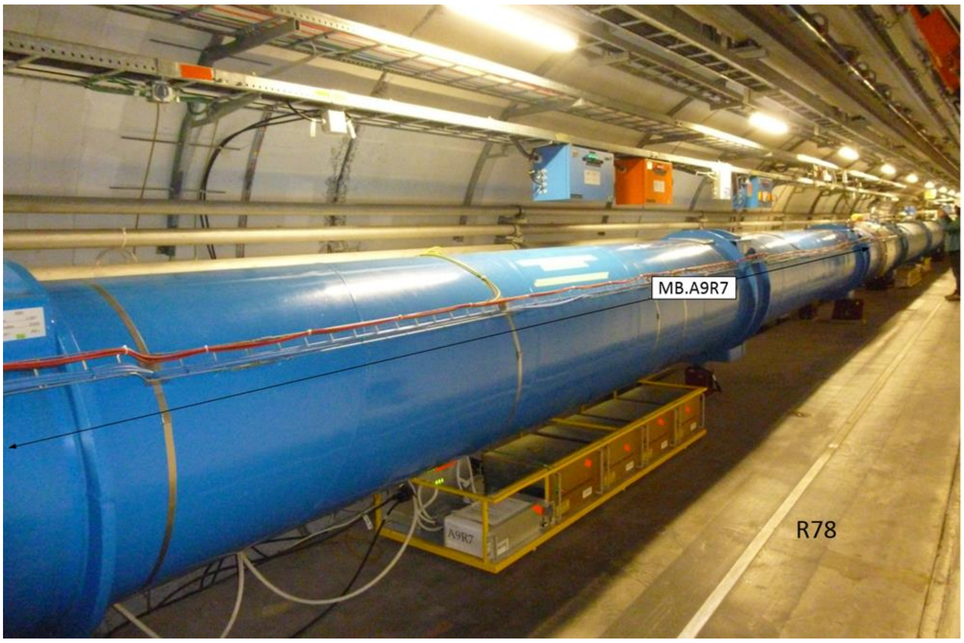

Figure 2 — Picture of area under change, 9R7 at R78 – present MB.A9R7 (18/02/2019)

2. REASON FOR THE CHANGE

The increased intensities of the proton and heavy-ion beams in the High-Luminosity (HL) LHC configuration require the installation of collimators in the cold DS region of the IR7 cleaning insertion to protect the downstream dipoles. Beam lifetime drops to 0.2 h may occur and cause energy depositions close or above the quench limit in the DS dipoles for the nominal HL-LHC beam parameters planned for Run IV (Table 1) and for a 7 TeV beam energy [3, 4]. Heavy-ion beams are expected to reach full intensity already after LS2 and potentially producing losses well beyond the quench limit for 0.2h BLT. Therefore, the HL-LHC project, with the approval of the CERN management, has included the installation of the 11 T dipoles with TCLDs already in LS2 as a critical item in its baseline. This choice was taken as there is no room left for the installation of TCLDs without replacing two 14.3 m long 8.33 T standard LHC main dipoles (MB) each with an assembly consisting out of a pair of 5.5 m-long 11 T dipoles making room for a central bypass cryostat (length 3.3 m) hosting the TCLD collimator (length 1 m).

Table 1: Nominal HL-LHC beam parameters, Run IV

	Number of bunches	Number of particles/bunch
Protons	2760	2.3e11
Ions	1248	2.1e8

This baseline was decided in 2016, after a re-baselining took place, at which the second 11 T dipoles in cell 10 was removed from the initial HL-LHC baseline. This re-baselining was followed by a massive simulation campaign to explore the optimum position of the remaining TCLD collimators (see for example [5, 6]). Two positions (MB.B8 or MB.A9) were identified as good candidate positions. Tables 2 and 3 present the uniform power densities in the most exposed magnets and the total power deposition in the cryogenic half-cells for these two positions and compares the results to no TCLD collimator installed (no change). The calculation method for the uniform power density is specified in [7] (called in this publication minimum quench power density). Please note that the presented peak power densities provided in Tables 2 and 3 are averaged over the cable radial width and are multiplied by the empiric factor of 3 to take into account uncertainties between energy deposition simulations of the multi-turn collimation cleaning process and the LHC measurements during previous beam-based quench tests.

The minimum power density to induce a MB quench was found to be 15-20 mW/cm^3 in the BFPP (bound-free pair production) quench test, which took place at 6.37 TeV [8]. This quench limit value was reconstructed by performing particle shower simulations based on the experimental conditions achieved in this test (20 second steady state losses). The value is however affected with some uncertainty as aperture imperfections in the beam screen could not be fully recreated in the simulations. Other quench tests were carried out with collimation losses using both proton and Pb beams [9]. In the later test a dipole quench at about 25-30 mW/cm^3 (values reconstructed in simulations). The losses exhibited different time profiles in the different tests, which affected the minimum power density needed to induce a quench. According to electro-thermal simulations, the minimum quench power density in mW/cm^3 can be a factor of two or more higher if the losses are rising (like in the collimation tests) than if the losses are constant in time (like in the BFPP quench test). This can possibly explain why the maximum power density was found to be somewhat higher for the Pb collimation quench test than for the BFPP test. It should nevertheless be stressed that a certain error margin needs to be taken into account when interpreting the power densities reconstructed in the simulations, considering the complex simulation setup needed. At the nominal LHC beam energy of 7 TeV these values are around 20% lower.

The expected 11 T dipole quench limit for a uniform power density is 70 mW/cm^3 (as relevant for comparison with Table 2) [10]. Please note that contrary to the quench limits of the MBs, which are based on beam based measurements under real conditions in the LHC, the values for the 11 T are based on (1) measurements of cable stack samples, (2) on short magnet models tests (not exactly of the same type as the 11 T) and on (3) calculations; as reviewed and summarized in [10]. Based on this review and the point of view of operating margin and stability, the 11 T dipole meets the requested resilience to heat load for both installation locations presented in Tables 2 and 3.

The cryogenic cooling capacity allows to extract ~200 W per 2-cells (Q7 to Q11); for a short time much higher heat loads can be sustained by using the heat capacity of the stored helium and extracting the heat once the heat load is again reduced. Taking into account the heat deposition as function of time, in all cases for protons and ions the magnets' temperature excursion can be contained below T_λ [11]; so as well both locations presented in Tables 2 and 3 fulfil the requested resilience.

From these tables, one concludes that the margin to quench improve for the downstream MBs and MQs (Nb-Ti magnets), in particular for ion runs, if the TCLD is installed in MB.A9 compared to MB.B8, allowing beam lifetimes of 0.2 h (but at the cost of higher losses for the 11 T dipoles [48 mW/cm^3 (proton runs, MB.A9) compared to 21 mW/cm^3 (ion runs, MB.B8)]. If the TCLD would be installed at MB.A8 beam lifetimes of 0.2 h could require a beam dump to not quench the Nb-Ti magnets for ion runs, or the use of other techniques like crystal collimation [12].

In view of the overall optimization goal to maximize the integrated luminosity, taking all information and the uncertainties into account, the HL-LHC management decided to install the 11 T dipole at MB.A9 [13].

Table 2: Uniform power density in SC coils in mW/cm^3 for 0.2 h and 1 h beam lifetime for different scenarios (no TCLD, TCLD installed at MB.B8 or MB.A9) [3]

		PROTONS					IONS				
		Cell 8/9			Cell 11		Cell 8/9			Cell 11	
TCLD position		*MB*	*MQ*	*11T*	*MB*	*MQ*	*MB*	*MQ*	*11T*	*MB*	*MQ*
No TCLD	0.2h	21	9.9	-	12	13	57	27	-	57	36
	1h	4.2	2	-	2.4	2.6	11	5.4	-	11	7.2
MB.B8	0.2h	6.6	8.1	11	8.7	13	5.4	15	21	36	33
	1h	1.3	1.6	2.2	1.7	2.6	1.1	3	4.2	7.2	6.6
MB.A9	0.2h	6.0	8.1	48	<0.3	<0.3	6.0	3.6	33	<0.003	<0.003
	1h	1.2	1.6	9.6	<0.06	<0.06	1.2	0.7	6.6	<0.0006	<0.0006

Table 3: Total power in cryogenic cells in W for 0.2 h and 1 h beam lifetime for different scenarios (no TCLD, TCLD installed at MB.B8 or MB.A9) [3]

		PROTONS						IONS					
		Half-cells						Half-cells					
TCLD position		*8*	*9*	*10*	*11* T	*CC*	*12*	*8*	*9*	*10*	*11* T	*CC*	*12*
No TCLD	0.2h	50	740	15	280-310	100	10	10	985	35	910-1015	270	25
	1h	10	148	3	56-62	20	2	2	197	9	182-203	54	5
MB.B8	0.2h	210	100	10	230-265	85	10	351	135	20	569-635	115	20
	1h	42	20	2	46-53	17	2	70	27	4	112-127	23	4
MB.A9	0.2h	51	475	3	2.1-2.2	<1	<1	9	758	<1	<1	<1	<1
	1h	10	95	<1	<1	<1	<1	2	152	<1	<1	<1	<1

3. DETAILED DESCRIPTION

It is foreseen to exchange the following two MBs:

- **MB.A9L7** (LBBRB.9L7)
- **MB.A9R7** (LBARA.9R7)

The cryo-magnets (LB) are installed at the following positions (virtual interconnect plane, upstream B1):

- **MB.A9L7** (LBBRB.9L7): distance from IP7: -323.629 m, distance from IP1 (DCUM): 19670.5334 m, half-cell 9.L7, called following **P7 left side**
- **MB.A9R7** (LBARA.9R7): distance from IP7: 307.969 m, distance from IP1 (DCUM): 20302.1314 m, half-cell 9.L7, called following **P7 right side**

In detail, the changes comprise the following:

P7 left side

- Removal of the present main dipole **MB.A9L7** (LBBRB.9L7, circuit RB.A67)
- Installation of the 11 T dipole full assembly at the MB place in type cold-mass type B configuration (only MCS corrector connected). The assembly is composed of two dipoles of equal bending strength and shorter magnetic length (Cryo-assembly A and B) and a bypass cryostat in the middle, providing cryogenic and electrical continuity between them.
- After that, installation of a new TCLD collimator between the two magnets, on the beam line 2 (internal beam, or passage side) will follow.

P7 right side

- Removal of the present main dipole **MB.A9R7** (LBARA.9R7, circuit RB.A78)
- Installation of the 11 T dipole full assembly at the MB place in type cold-mass type A configuration (both MCDO and MCS corrector connected): Cryo-assembly A and B, and a bypass cryostat in between.
- After that, installation of a new TCLD collimator between the two magnets, on the beam line 1 (external beam, or QRL side) will follow.

Layout drawings LHCLSS__0029/LHCLSS__0030 (LHC layout for the DS region at point 7) show the present situation in LHC. LHCLSSH_0013/LHCLSSH_0014 (HL-LHC layout for the same zones) show the situation after the installation of the TCLD collimator and the two short 11 T dipoles and replace the before mentioned drawings after LS2. Figures 3 and 4 show the section of the LHC layout for P7 left before and after the change. Detailed layouts are presented in [13].

The components to be installed (Table 1), to be kept (Table 2), to be displaced (Table 3) or to be removed (Table 4) are listed below.

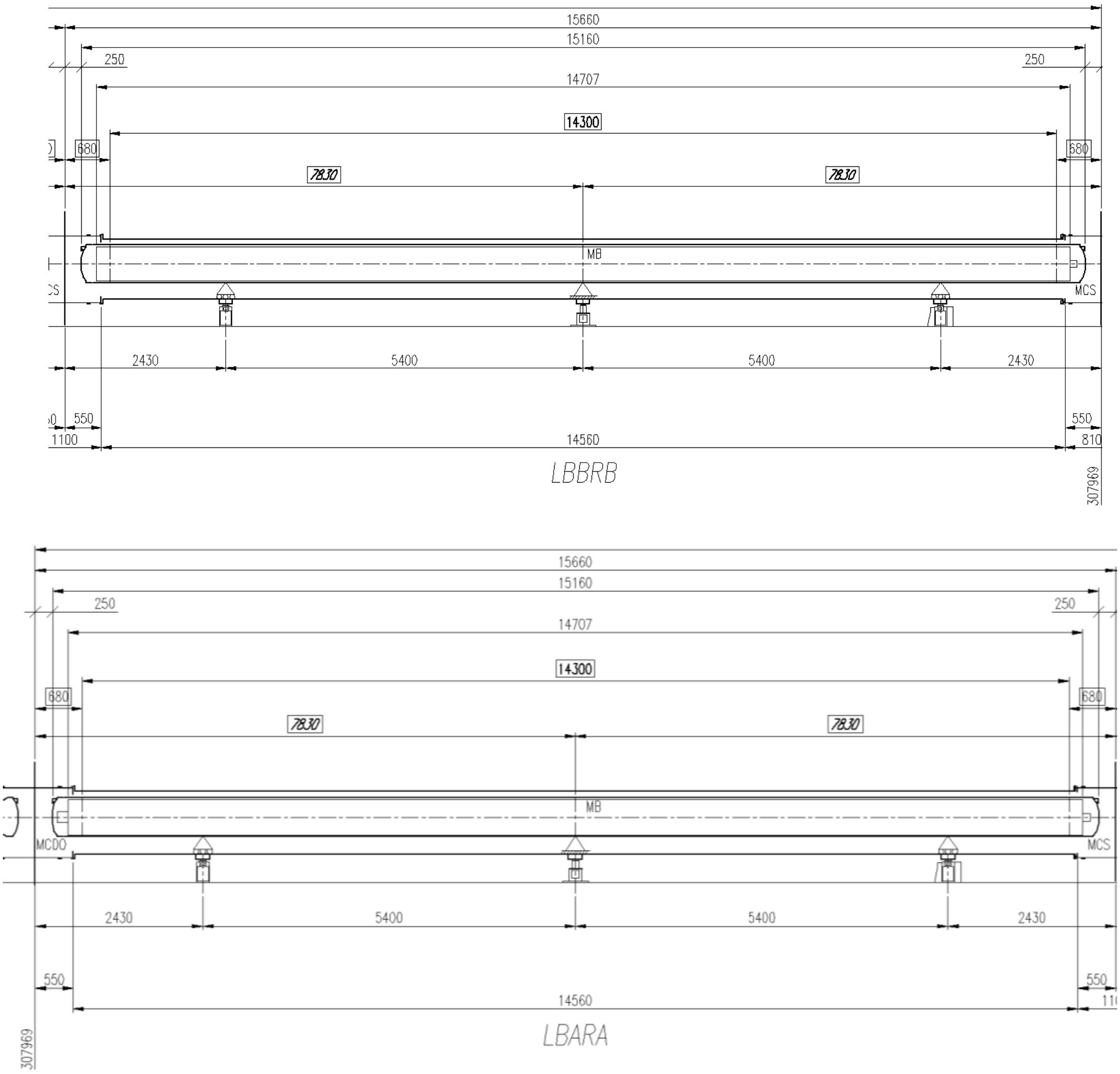

Figure 3 - Section of LHC layout for P7 left (from LHCLSS__0029, top) and P7 right (from LHCLSS__0030, bottom) – Replaced magnet.

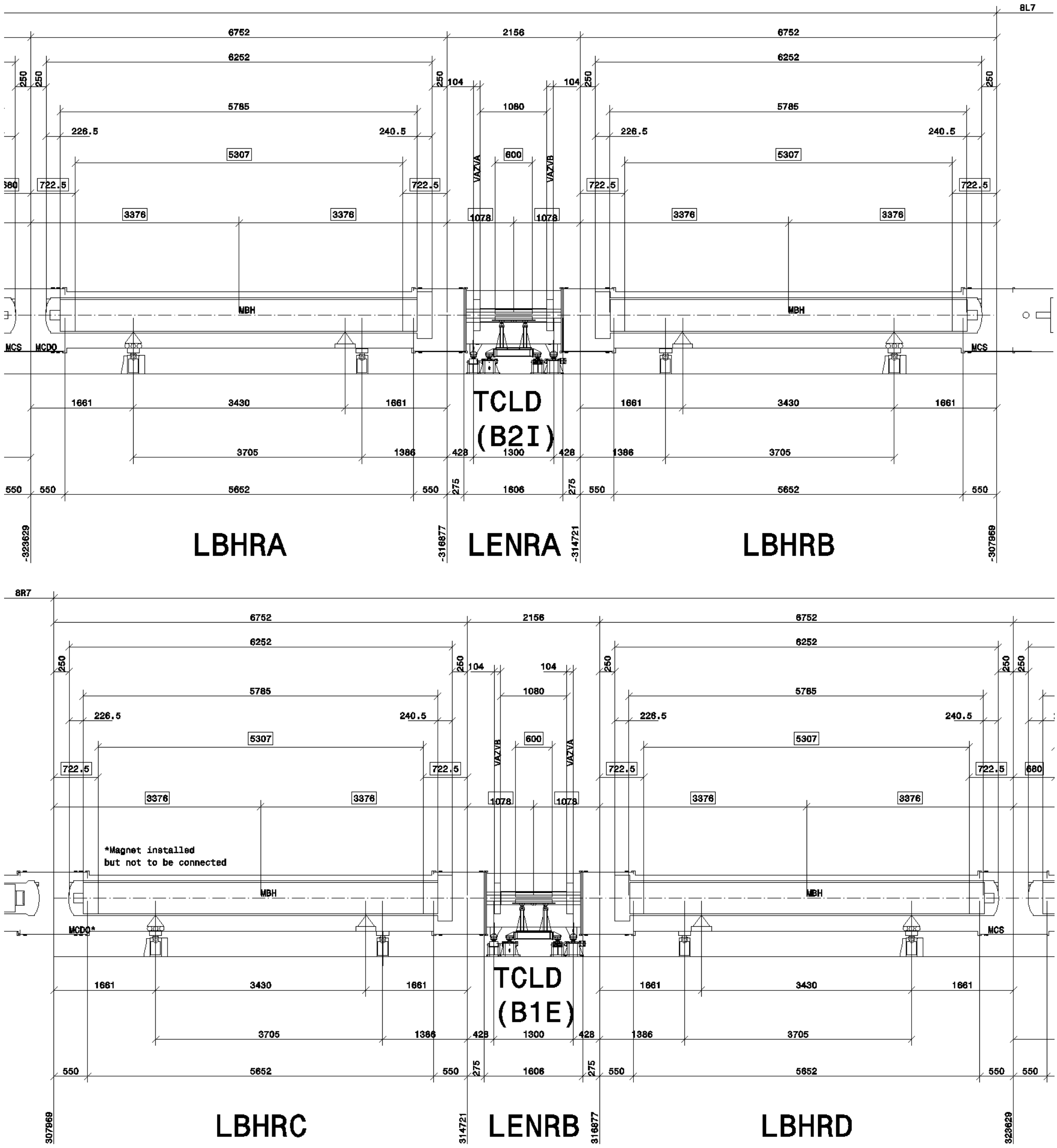

Figure 4 - Section of HL-LHC layout for P7 left (from LHCLSSH_0013, top) and P7 right (from LHCLSSH_0014, bottom)– New components

Table 4 - Components to be installed

Equipment name	DCUM [m]	IP7 [m]	Comments
LBHRA – 11T dipole **LENRA** – Bypass **LBHRB** – 11T dipole	19670.5334 m 19677.2854 m 19679.4414 m	– 323.629 m – 316.877 m – 314.721 m	Composed of 2 cryoassemblies + 1 bypass cryostat.
2 DYPB double racks	-	-	1 DYPB under MB.B9L7 and 1 DYPB under MB.B10L7. See 2.4.5, [13]
1 Power Converter for 11T.9L7	-	-	Installation of a new PC named RYABA01 at RR73. See 2.4.4, [13]
Water connection for PCs	-	-	For water-cooling of the new PC at RR73. See 2.4.1, [13]
2 crates for QDS + **trim leads protection** Equipment	-	-	To be installed at RR73. See 2.4.5, [13]
3 BLMs at L7			See 2.4.8, [13]
Limited stay areas at L7	-	-	See 2.4.6, [13]
DN200 valves	-	-	See 2.4.6, [13]
LBHRC – 11T dipole **LENRB** – Bypass **LBHRD** – 11T dipole	20302.1314 m 20308.8834 m 20311.0394 m	307.969 m 314.721 m 316.877 m	Composed of 2 cryoassemblies + 1 bypass cryostat.
2 DYPB double racks	-	-	1 DYPB under MB.A8L7 and 1 DYPB under MB.A10L7. See 2.4.5, [13]
1 Power Converter for 11T.9R7	-	-	Installation of a new PC named RYABA01 at RR77. See 2.4.4, [13]
Water connection for PCs	-	-	For water cooling of the new PC at RR77. See 2.4.11, [13]
2 crates for QDS + **trim leads protection** Equipment	-	-	To be installed at RR77. See 2.4.5, [13]
3 BLMs at R7	-	-	See 2.4.8, [13]
Limited stay areas at R7	-	-	See 2.4.6, [13]
DN200 valves	-	-	See 2.4.6, [13]

Table 5- Components to be kept

Equipment name	DCUM [m]	IP7 [m]	Comments

Table 6 - Components to be displaced

Equipment name	DCUM [m]	IP7 [m]	Comments
DYPQ.9L7			Present under MB.A9L7. To be displaced under MB.B8L7
Electrical boxes	-	-	Installed on cable trays. See [14] and 2.4.9 [13],. Electrical distribution)

Table 7 - Components to be removed

Equipment name	DCUM [m]	IP7 [m]	Comments
MB.A9L7 (LBBRB.9L7)	19670.5334 m	– 323.629 m	
DYPB.A9L7			Protecting present MB.A9L7
RYSA01 rack at RR73	-	-	It will be replaced by the new RYABA01 (11T Power converter)
MB.A9R7 (LBARA.9R7)	20302.1314 m	307.969 m	
DYPB.A9R7			Protecting present MB.A9R7
RYSA01 rack at RR77	-	-	It will be replaced by the new RYABA01 (11T Power converter)

3.1 INTEGRATION

The integration is described in detail in the document [13].

3.2 BEAM DYNAMICS

The bending angle of the beam is kept the same thanks to the same integrated field generated by the pair of 5.5 m-long 11 T dipoles as by a standard main dipole magnet (MB). The same integrated field is achieved by powering the 11 T dipole pair in series with the MBs and by using a trim power supply, so no orbit distortions will be generated due to differences in transfer function of the main and the 11 T dipoles during the energy ramp.

The field stability is similar, as the 11 T dipoles are connected in series with the MBs, so the main current in all magnets is identical during standard operation. The trim power converters have a marginal impact. Flux jumps are too slow for having a negative impact on the emittance and the orbit [16, 17].

The field quality is worse than for that of the MBs, in particular the sextupole component b_3 is larger. The latest field quality table of the 11 T dipoles can be found in [15]. Beam dynamics studies [18] have shown that the expected field quality is such to leave dynamic aperture essentially unaffected, both at injection and collision energy, given the limited number of magnets which will be installed.

The same type and number of spool pieces as currently installed in the MBs will be installed in the 11 T dipoles (LBBRB.9L7: MCS, for symmetry reason a MCDO will be installed but not connected to the circuit to mimic the type B dipole; LBARA.9R7: MCS and MCDO).

Unlike the main dipoles, the 11 T magnets are straight. The exact installation positon taking into account the sagitta is currently being assessed in the WG alignment [19].

3.3 VACUUM MODIFICATIONS

In order to provide beam vacuum continuity of the 11 T full assembly, the continuous beam line of the replaced dipole magnet must be segmented and adapted to accommodate the functioning of the TCLD collimator and the 11 T magnets. The installation of the TCLD collimator, operating at room temperature, imposes a new sectorization of the vacuum lines and new transitions between cold and warm vacuum lines. The improved pumping strategy for these new vacuum sectors is proposed in [20]. All changes of the vacuum layout are defined in [21].

Inside the 11 T magnets (LBH type) the standard LHC-type beam screens will be installed for both beam lines (cold bore inner diameter 50mm). Regarding the bypass cryostat (LEN type) there are two different configurations, one for each beam line, depending if it is the collimated or the non-collimated line.

For the collimated line, there will be one bellow to ease its mounting/dismounting and one sector valve installed on each side of the TCLD. The sector valves are then connected to the cold-warm transitions (short and long versions, located upstream and downstream respectively) and followed by the standard Plug-in-Module (PIM). The collimator itself will represent an added vacuum sector, described in detail within the TCLD ECR [2] after on-going tests. A vacuum port (LHCVSTB_0010 – position5) is integrated in the cold/warm transition, between the sector valves and the continuous cryostat, to allow the RF ball tests.

For the non-collimated line, a new concept of conduction cooled copper cold bore has been developed to reduce the equipment needed on this line of the bypass cryostat. It will be thermalized at both of extremities by two hoses routed from the M3 line, feeding superfluid helium at 1.3 bar to the collars brazed around the line. The copper cold line is linked to the PIMs at the extremities. A standard LHC-type beam screen is inserted in the cold line. To accommodate all the described equipment within the existing space, special

short beam screen bellows had to be design and manufactured. The additional cryogenic instrumentation is described in section 3.4.
The insulation vacuum continuity is ensured by the LEN cryostat.

3.4 CRYOGENICS MODIFICATIONS

The bypass cryostat placed between two 11 T dipole cryostats causes a significant increase of the longitudinal hydraulic impedance in the insulation vacuum-space compared to today's installation. In case of a 30 kg/s cold helium flow from the cold mass into the insulation vacuum space, as identified as Maximum Credible Incident (MCI) in [22], a sufficient number of safety valves are installed to limit the cryostat pressure to 1.5 bar. The present scheme, implemented after the incident of 19th September 2008 and revised in LS1 is summarized in [23, 24]. An investigation whether this MCI-discharge flow occurring on one side of the cryogenic bypass can be at least partly shared with the other side, without introducing an excessive pressure drop, showed that such sharing is insufficient [25]. Therefore, each side of the cryogenic bypass is to be considered as an individual hydraulic sector with respect to MCIs and it must be possible for the full flow to be discharged by safety valves on either side of the bypass.

In addition, to avoid multiple helium clouds in case of an incident when personnel access is allowed in the tunnel (during low current powering, so-called "phase I" [23]), one SV per vacuum subsector opens at a low pressure (so-called unsprung SV), allowing evacuation of up to 1 kg/s of helium via a single port. The additional hydraulic impedance of the bypass cryostat increases the maximum internal pressure for such a 1 kg/s discharge. An investigation whether this MCI-discharge flow occurring in the dispersion suppressor cryostat equipped with bypass cryostat showed that the internal pressure slightly exceeds the 80 mbar opening pressure of the sprung loaded DN200 SV in the hydraulic sector opposite to the location of the unsprung SV [25]. A simple solution to increase the opening pressure of the DN200 SV by applying a second spring has been verified [26]. Furthermore, the two DN90 SV with opening pressure of 67 mbar shall be removed from the vacuum subsector.

The cold mass complies to the functional requirements provided in [27]

The insulation vacuum protection scheme at LHC IR 7 DS vacuum sector before and after LS2 is summarized in Tables 8-11. The change concerns two 11 T dipole magnets (MBH), one by-pass cryostat (LEN), one additional DN200 SV to install on the MB between Q7 and Q8, removal of the DN90 SV at Q7 and Q9, doubling of DN200 springs in the zone Q11 to LEN. The valve without spring is displaced from cell 10 to cell 7.

Table 8: LHC IR7 LEFT Insulation vacuum protection scheme in sector 6-7 as installed on 31st of January 2019

	Q11	LE	MB	MB	Q10	MB	MB	Q9	MB	MB	Q8	MB	MB	Q7	DFBA
DN230															
DN200*				1											
DN200		1	1			2	1		2	1		2	1		
DN200**															
DN160															
DN100															
DN90								1						1	
D65															
Limited stay															

*no spring loading, **double spring loaded

Table 9: LHC IR7 LEFT Insulation vacuum protection scheme in sector 6-7 as after installation of the 11 T dipole (MBH)

	Q11	LE	MB	MB	Q10	MB	MB	Q9	MB	MBH	LEN	MBH	Q8	MB	MB	Q7	DFBA
DN230																	
DN200*															1		
DN200												2		2	1		
DN200**		1	1	1		2	1		2	1							
DN160																	
DN100																	
DN90																	
D65																	
Limited stay																	

*no spring loading, **double spring loaded

Table 10: LHC IR7 RIGHT Insulation vacuum protection scheme in sector 7-8 as installed on 31st of January 2019

	DFBA	Q7	MB	MB	Q8	MB	MB	Q9	MB	MB	Q10	MB	MB	LE	Q11
DN230															
DN200*												1			
DN200			2	1		2	1		2	1			1	1	
DN200**															
DN160															
DN100															
DN90		1						1							
D65															
Limited stay															

*no spring loading, **double spring loaded

Table 11: LHC IR7 RIGHT Insulation vacuum protection scheme in sector 7-8 as after installation of the 11 T dipole (MBH)

	DFBA	Q7	MB	MB	Q8	MBH	LEN	MBH	MB	Q9	MB	MB	Q10	MB	MB	LE	Q11
DN230																	
DN200*				1													
DN200			2	1		2											
DN200**								1	1		2	1		1	1	1	
DN160																	
DN100																	
DN90																	
D65																	
Limited stay																	

*no spring loading, **double spring loaded

Additional cryogenic instrumentation will be implemented during LS2. A total of seven temperatures sensors (CERNOX) and two flowmeters (Coriolis) will be installed at P7 right side after having installed the 11 T dipole magnet [28]. No additional instrumentation at P7 left side will be installed. This choice was taken because the beam screen heat load on the right side is larger. Figure 5 shows the instrumentation in this half-cell.

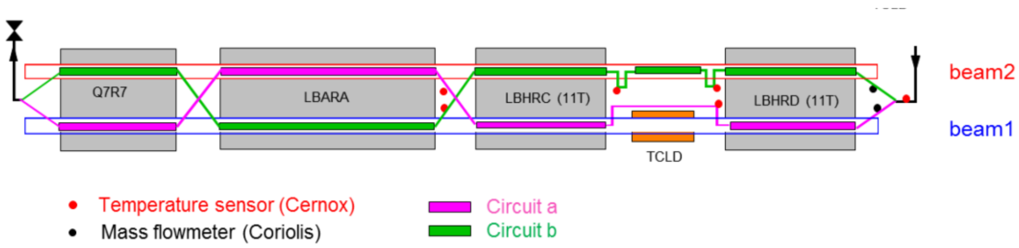

Figure 5 – Instrumentation for the 11 T dipole, P7 right side [28].

3.5 GEOMETRY AND ALIGNMENT MODIFICATIONS

The installation of the 11 T dipole full assembly requires the alignment of two 11 T dipoles, the bypass cryostat and the TCLD collimator compared to previously only one MB magnet. In detail, the following operations have to be performed:

1. The marking on the floor of the beam points, jacks heads position of the non-standard 11 T dipoles but also the beam points and component axis of the bypass cryostat and of the new TCLD collimator is required. A specific care will be brought to the jack configuration of the dipoles, as not standard.
2. 12 jacks per 11 T dipole full assembly will be installed.
3. EN-SMM-ASG will align the jacks' heads at their nominal position, prior to the installation of any component.
4. The 11 T dipole magnets will be installed.
5. An initial alignment of the dipoles will be carried out with respect to the adjacent cryo-magnets.
6. The bypass cryostat will be installed and the TCLD collimator will be inserted as last component to be installed.
7. The alignment of the TCLD and cryo-bypass will be carried out from the both 11T adjacent dipoles. Please note that during the smoothing activities of the cryo-magnets in the LHC (end of LS2), if one of the 11T magnets is re-aligned (vertical or radial), the components between the both 11T magnets (TCLD and cryo-bypass) may also need to be re-aligned.
8. After this pre-alignment, the 11 T dipole full assembly smoothing w.r.t. the adjacent components will be performed once all interconnections are closed, and the sector has been cooled down during the regular arc smoothing activity.
9. Roll measurements can only be performed by adding an inclinometer on a specific cylinder interface located on the plate that supports the survey socket on the tunnel transport side and on the double jack side.

To do all alignment operations described above, the MAD-X survey file providing the beam positions of the components must be available at least two months before any survey activity in the LHC tunnel, this will be possible only if the LHC layout database will be updated with the needed information at least a month in advance the deadline for the delivery of the MAD-X survey file. Drawings giving the positions of the jacks heads with respect to the component beam points must be available at least two weeks before the jack marking in the LHC tunnel.

3.6 MAIN DIPOLE CHAIN AND TRIM CIRCUIT

The modified circuit layout of RB.A67 (with trim circuit **RTB9.L7**) and RB.A78 (with trim circuit **RTB9.R7)** is shown in Figures 5 and 6. A detailed description of the circuits is provided in [29, 30], Section 2.1-2.7. The RB circuit characteristics before and after the change are summarized in Table 12. For the circuit RB.A78 the 11 T dipole full assembly will be placed after the second energy extraction system, creating a little dissymmetry in the RB circuit.

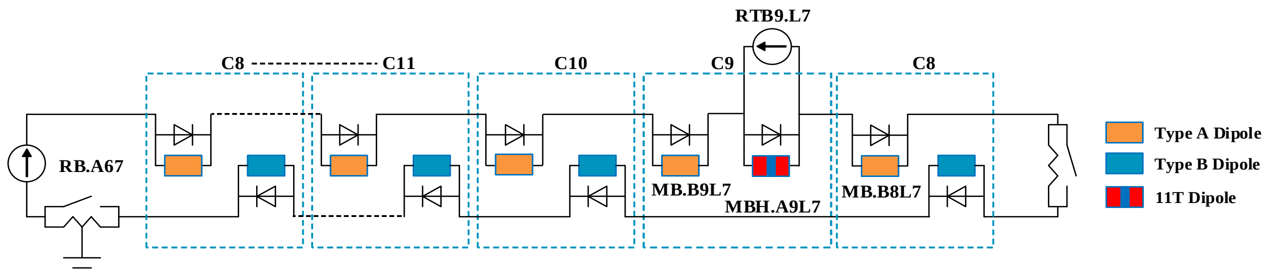

Figure 5 - Main dipole circuit RB.A67 configuration for the HL-LHC with the 11 T trim power converter.

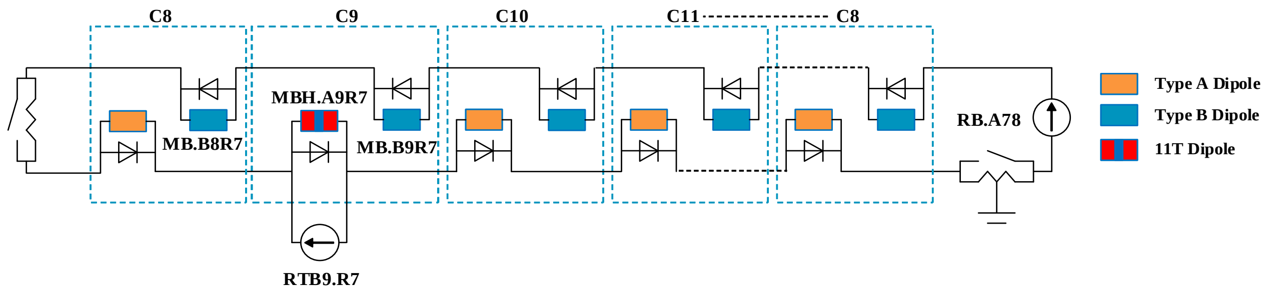

Figure 6 - Main dipole circuit RB.A78 configuration for the HL-LHC with the 11 T trim power converter.

Table 12 - RB circuit characteristics in the current LHC configuration and after the introduction of 11 T dipole full assembly for circuits RB.A67 and RB.A78, updated from [1].

	Circuit	LHC	HL-LHC
Maximum required RB PC voltage	RB.A67, RB.A78	171 V	171.6 V
Total RB circuit inductance	RB.A67, RB.A78	15.708 H	15.734 H
RB circuit DC cable resistance	RB.A67, RB.A78	1 mΩ	1 mΩ
RB circuit crowbar resistance	RB.A67, RB.A78	0 mΩ	0 mΩ
RB circuit energy extraction resistance	RB.A67, RB.A78	140 mΩ	140 mΩ
RB circuit natural time constant	RB.A67, RB.A78	15700 s	15740 s
Energy extraction time constant	RB.A67, RB.A78	112 s	113 s
Maximum required Trim PC voltage	RTB8.L7, RTB8.R7	NA	5V
Trim circuit inductance	RTB8.L7, RTB8.R7	NA	0.132 H
Trim circuit DC cable resistance	RTB8.L7, RTB8.R7	NA	30 mΩ
Trim circuit crowbar resistance	RTB8.L7, RTB8.R7	NA	50 mΩ
Trim circuit natural time constant	RTB8.L7, RTB8.R7	NA	10 s
Maximum common voltage of the trim circuit in case of energy extraction (ultimate energy)	RTB8.L7, RTB8.R7	NA	431 V
Maximum common voltage of the trim circuit in case of energy extraction + earth fault (ultimate energy)	RTB8.L7, RTB8.R7	NA	910 V

3.7 POWER CONVERTERS AND SERVICES

For the operation of the 11 T dipole magnets the trim di-polar circuit power converters (±250 A) have to be added. The current profile of the trim power converters is presented in [30].

3.7.1 RB power converter

No modifications are applied to the RB power converters, except setting the expected circuit inductance in the regulation to the slightly higher value: 15.734 mH vs 15.708 mH.

3.7.2 Hardware requirements

Two additional HCRPMBE (R2E-HL-LHC600A-10V) power converters will be added to the service galleries RR73 to power RTB9.L7 and RR77 to power RTB9.R7. A detailed description of the power converter functional requirements is detailed in [31]. The power converters racks will replace the RYSA01 in both RR73 and RR77.

3.7.3 Power converters control

The 11 T trim power converters will be controlled by FGCLite. They will be connected to the already existing WorldFIP network in RR73 and in RR77. For 11 T trim power converters, one agent will be added to the CFC-SR7-RL7A network in RR73 and another agent will be added to CFC-SR7-RR7C network in RR77. The required performance in terms of precision and stability is defined in [29].

3.7.4 Power converters services

The power converters will require the following services as indicated in Section 4.2:

- AC cabling per converter: 3P+N 20 Arms from ERD with a terminal (model Schneider A9N15658) and 3P+N 2 Arms from EOD with a terminal (model Schneider A9N15656).
- DC cabling per converter: 2 x 50 mm^2 per polarity
- Demineralized water cooling: 4 l/min at 3.0 bar of differential pressure drop

Two cables in parallel are used for the powering of the circuit, by means of 2 current leads of the 120 A LHC type per polarity (see section 3.12 for more details on PIC and section 3.13 for the DIC document number).

3.7.5 Power converter interface with PIC

The connection to the power converter will be done via a standard 12-pin female Burndy connector (the DIC number is reported in section 3.13).

3.8 Quench Detection System (QDS) modifications

For the protection of the 11 T dipoles, newly developed universal quench detection system (uQDS type) adapted to the specific properties of Nb_3Sn superconducting magnets (uQDS type) will be deployed. In addition, dedicated DAQ systems for the supervision of the quench heater circuits (DQHSU) will be provided.

3.8.1 Hardware

To assure the quench detection system, two crates are needed per IP side and will be installed in the service galleries RR73 (left side) and RR77 (right side). A detailed description of the integration of these racks is provided in [13].

The dipole quench detection crates DQLPU.A9L7 and DQLPU.A9R7, which are installed in protection racks DYPB.A9L7 and DYPB.A9R7, will be dismantled and removed from the LHC tunnel.

3.8.2 Location

The QDS for the protection of the 11 T dipoles and the associated quench heater circuit supervision unit (DQHSU) will be located in underground areas RR73/RR77 using the remaining free space in QPS protection racks DYPG01=RR73 and DYPG01=RR77.

3.8.3 Interlocks

This non-standard QDS will be integrated into the existing QPS internal current loop. While the connection to the powering interlock controller (PIC) will not change, it is foreseen to update the QPS quench loop controllers for circuits RB.A67 and RB.A78 in order to achieve a faster reaction time.

3.8.4 Controls

The physical layout of the QPS fieldbus needs to be slightly modified. This concerns segments CBW.IP7.DR7H, CBW.IP7.DL7J, CBW.IP7.DT7A and CBW.IP7.DT7F. The changes concerns only the number and position of field-bus clients; it does not affect any other active equipment like repeater or front-end computers.
The QPS software layer stack and the LHC circuit synoptic need to be updated to be able to interact correctly with the newly installed devices. In particular, this will require the implementation of several new application-programming interfaces (API) and the definition of the corresponding set of signals.

3.9 New Quench Protection System (nQPS) modifications

The DQLPU type S protection crates will not need any type of relocation since they are not affected for the new location of the 11T cryo-assemblies.

3.10 Changes to the racks containing the heater discharge units

For the protection of 11 T magnets, two non-standard QPS racks will be installed in the machine tunnel per IP side (underneath the cryostats). A new, non-standard design was established, to consider that the quench detectors will be located in the RRs (see Section 3.8) and to accommodate the 16 quench heater power supplies per side instead of the previously installed 4 standard LHC MB quench heater power supplies. The quench heater power supply will accommodate redundancy in the powering of the F3 & F4 UPS distribution lines.

A detailed description of the integration of these racks is provided in [13].

3.10.1.1 DQHDS firing speed

The response time of the DQHDS units in firing is 2ms, which is considered sufficient.

3.10.1.2 Redundancy configurations

Since the full 11 T magnet cannot withstand the loss of more than two out of sixteen DQHDS units, powering redundancy must be incorporated. To ensure redundancy, each rack is powered with four F3 and four F4 AC inputs together with twice four circuit breakers per rack. In addition, each DQHDS unit will be modified in such a way that its trigger circuit will have a redundant powering from F3 and F4. However, the capacitors will still be energized by either F3 or F4. The powering requirements are addressed in the DIC.

Monitoring of the proper connections of the quench heater discharge cables to the magnet IFS will be performed.

3.10.1.3 Rack containing the heater discharge units

A new rack type upgrading the current DYPB rack had to be designed to allow for installing 16 quench heater power supplies and allow maintenance during LHC operation. In addition to this, the DQHDS units must be upgraded to be compatible with the availability requested by the protection of the 11 T dipoles.

3.10.2 Location

The non-standard QPS racks will be placed at (see the grey boxes in Figure 7):

- L7: 1 rack under MB.B10L7 + 1 rack under MB.B9L7;
- R7: 1 rack under MB.A10R7 + 1 rack under MB.A8R7.

Four new racks will be installed in the machine. One spare unit will be manufactured.

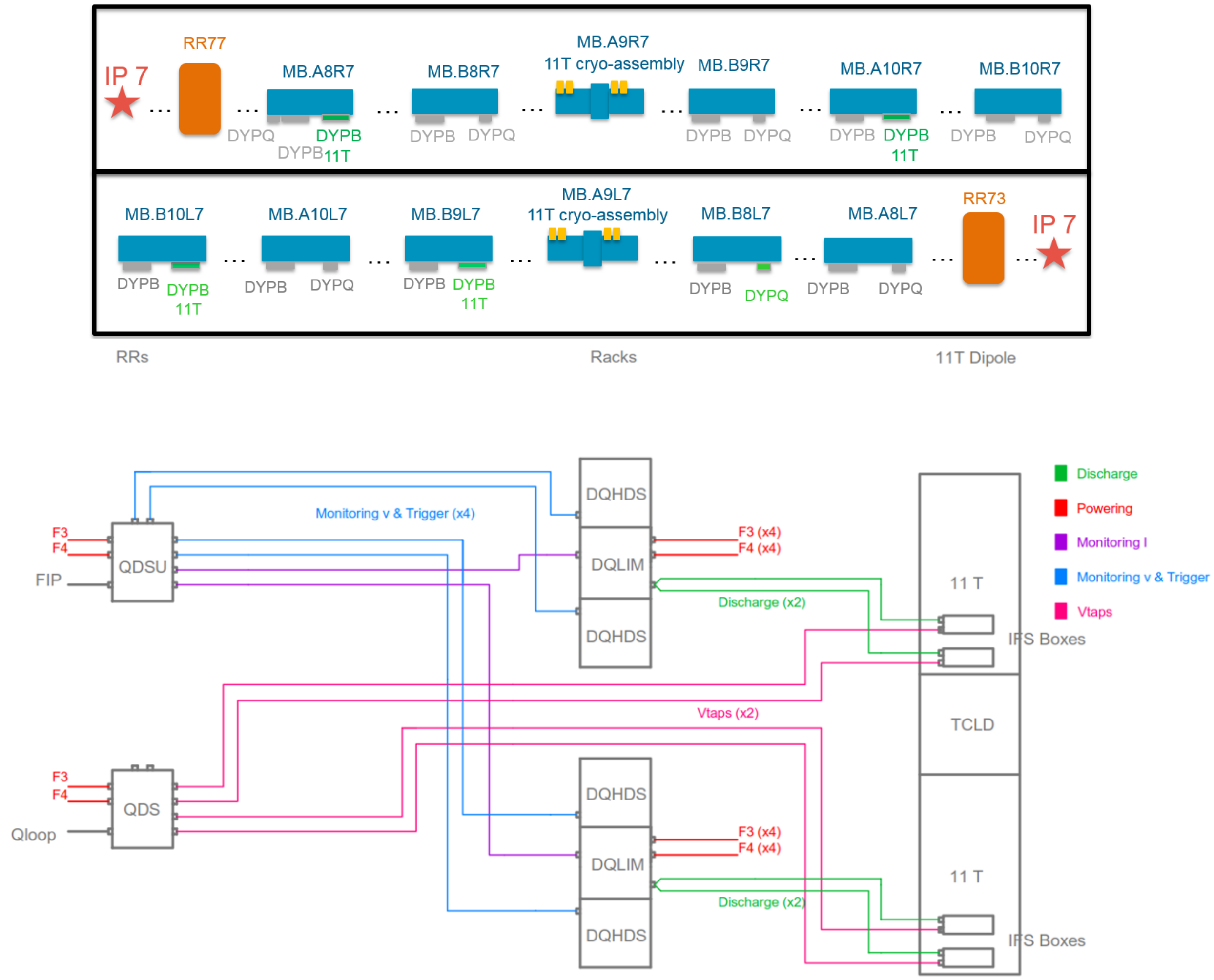

Figure 7 - Location of the new DYPB for the 11 T dipoles.

3.11 Powering Interlock System (PIC)

The Powering Interlock System (PIC) [31] is designed to ensure nominal conditions for circuit powering and provide the permission for powering the different electrical circuits with superconducting magnets installed around the LHC. For this, it interfaces power converters, quench detection systems, technical services (AUG, UPS, cryogenics, etc.)

and is a client of the Beam Interlock System (BIS) in order to request a beam dump when necessary. The two new 11 T dipoles will be connected in series with the RB.67 and RB.78 main dipole circuits requiring a trim power converter each, which have to be connected to the PIC. The interlock requirements of the 11 T circuit and its trim are summarized in Table 13

Table 13 - Interlock requirements

Interlock case	**PIC Action on RB Circuit**	**PIC Action on Trim Circuit**	**Beam Dump[1]**
Quench in RB circuit	Fast Power Abort	Fast Power Abort	Yes
Powering Failure in RB Circuit	Slow power Abort	No action	Yes
Powering Failure in Trim Circuit	No action	Slow Power Abort	Yes
QDS trip in the trim current leads	No action	Fast Power Abort	Yes
Switch opening request by RB PC	Fast Power Abort	Fast Power Abort	Yes
Cryo-failure	Slow Power Abort	Slow Power Abort	Yes

[1]The trim circuit will be considered as essential from the PIC side, which means unmaskeable at the BIC level.

3.11.1Hardware

The hardware interfaces of the PIC are standardized and are defined according to the type of electrical circuit. There are currently 5 different listed types (A, B1, B2, C, D) [32] grouped into 4 different patch panels (CIPPA, CIPPB, CIPPC, CIPPS). Since the configuration of a PIC is generic, there are some hardware interfaces that remain unused. For the two PIC in P7, the current interface configuration contains a free "B1 type" hardware interface on the CIPPS patch panel, which will be used to connect the new 11 T trim power converters. Moreover, the quench loop of the trim circuits will have the peculiarity of being connected to the QDS dedicated for the surveillance of the trim current leads (see Section 3.12, Protection of trim current leads)).

The proposed implementation will fulfil the requirements summarized in Table 6:

- If a quench in the RB circuit or an EE switch opening occurs, a general fast power abort action on both PICs on the odd and even side will be taken through the global protection mechanism.
- If a powering failure occurs, a slow power abort action will be taken only on the faulty circuit (RB or Trim).
- If a failure is detected on the current leads of the Trim circuits, a fast power abort of the trim circuits will be triggered.
- A cryo failure will cause a slow power abort of both RB and Trim circuit because the same status of the Cryo interlock is sent from a unique Cryo PLC to both arc PIC.
- For protection of the trim circuit bus-bars, the trim bus-bar supervision is added on the QDS of the 11 T, that means in case of a quench of the trim bus-bar the firing of the quench heaters of the 11 T dipole will be triggered and a fast power abort of the main dipole circuit will be performed [33].

As stated in Table 6 and confirmed in [34] the beam is dumped in all failure scenarios.

3.11.2 Configuration

The LHC main dipole circuits have the feature of being interfaced with the two adjacent PIC of the arcs (even and odd), sharing the same quench loop, and their power converters located on the even side. The new 11 T trim power converters will be located at the odd side of the arc (RR73 and RR77) and connected to the corresponding PIC as independent circuits.

3.12 Protection of trim current leads

The trim circuit (RTB8) for each of the 11 T dipoles will be powered through a set of 2 x 2 resistive current leads. The protection of the four trim leads will require monitoring of the lead voltages and currents. These signals will be evaluated by a standard HL-LHC quench detection system (uQDS), which initiates the necessary action e.g. a fast power abort of the concerned trim circuit.

3.12.1 Hardware

The additional quench detection crates need to be installed inside RR73/RR77 (ground floor). There is not enough space to integrate these units in protection racks DYPG01=RR73 and DYPG01=RR77. For the additional space, the adjacent half rack DYPIB01 (shared with the PIC half rack CYCIP01) will be used.
For the measurement of the lead currents, current sensors of the Hall type and clamped to the power cables will be installed in RR73 and RR77.

3.12.2 Interlocks

The new QDS for the trim current leads needs to be integrated into the hardwired interlock loop for the trim circuits.

3.12.3 Controls

As for the changes above, the QPS software layer stack and the LHC circuit synoptic need to be updated accordingly. In this case, this concerns as well the configuration of the PIC.

3.13 Cabling

Detailed DICs (reference: RQF0908671 (instrumentation), RQF0888406 (PIC), and RFQ0981328 (powering)) have already been prepared and sent to EN-EL. Another WorldFIP fieldbus extension for the trim power converters is requested to BE-CO (RQF0809614). Accordingly, all the cabling concerning the new racks (discharge, monitoring, triggering, control, etc) needs to be installed.
The installation will require the respective set of instrumentation, signal, and hardware trigger and interlock cables. The default QPS interlock cabling traversing the 11 T assembly will need to be modified.
The nQPS instrumentation and interlock cabling need to be modified. All cables going through the 11 T assembly must be re-routed to one of the cables trays on the tunnel wall to not interfere with maintenance operations of the collimators.
Instrumentation cables linking the current lead feed through box with the quench detection crates have to be installed. In addition, there will be the signal cables for the current sensors and the interlock cables, which are local to RR73/RR77.
The nQPS crates below the dipoles located in A9 (both sides), will be moved to a position below A10 and various cables will be re-installed.
Moreover, there is today a DYPQ rack located under MB.A9L7 that will be moved under MB.B8L7. This requires consequently new cabling between the quadrupole cryostat and the new position of the rack (see Figure 7).
All cabling for other required equipment is summarized in the integration report [13] and the list of cables to be modified is summarized in [35].

3.14 Organization of the work during LS2

During LS2 each equipment owner is in charge of the installation of their own equipment. DISMAC will be in charge of the installation and connection of the 11T dipoles full assembly. The detailed procedures for the installation and connection will be given to the DISMAC team. An onsite coordination for the whole activities related to the 11 T dipole will be guarantee by WP11 through the activity technical coordination of WP11 (Daniel Schoerling). The role description is provided in [36].

4. IMPACT

4.1 IMPACT ON ITEMS/SYSTEMS

The following drawings and documents have to be updated.

LHC Layout	LHCLSS___0029 - IR7 left, cells C8.L7 TO C11.L7 LHCLSS___0030 - IR7 right, cells C8.R7 TO C11.R7 These layout drawings will become obsolete.
Updated layout drawings	LHCLSSH_0013 - IR7 left, cells C8.L7 TO C11.L7 LHCLSSH_0014 - IR7 right, cells C8.R7 TO C11.R7
Differential layout drawings	LHCLJ_7U0085 - Differential Layout C9L7 LS2 LHCLJ_7U0087 - Differential Layout C9R7 LS2
Interconnection layout	LHCQQ_IG0033 – DS zone interconnections, type definition LHC-LI-ES-0017 – LHC interconnections naming and position convention
Electrical circuits	LHCLSD7_0002 – Electrical diagram of LHC magnets – left of IP7, C19.L7 TO C7.L7 LHCLSD7_0004 - Electrical diagram of LHC magnets – right of IP7, C19.R7 TO C7.R7 Equipment Layout LHCEY_7008 and LHCEY_7001 to be updated with the new racks in RR73 and RR77.
Cryogenic layout	LHCLSQR_0032 – P&I diagram of DS7 left LHCLSQR_0033 – P&I diagram of DS7 right
Vacuum layout	LHCLSVI_0020 – Schematic layout vacuum instrumentation, LHC arc and dispersion suppressor LHCLSVI_0031– Schematic layout insulation vacuum instrumentation, IP7 right and left
Main dipole chain	Circuits RB.A67 and RB.A78 will be modified. Table 5 provides a comparison of the parameters before and after the change.
Cryomagnet documentation	LHC-LBA-ES-0011- Cryodipole types arcs and dispersion suppressors Q8 To Q34 - Equipment codes and part identification LHC-LI-ES-0001 - Arc Cryomagnet Extremities LHC-LE-ES-0001 - Connection cryostats for LHC Dispersion Suppressors (DS) LHC-LE-ES-0002 - Instrumentation in the Connection cryostat (LE)
MP3	Hardware commissioning powering tests procedures have to be updated and established QPS class and failure scenarios have to be reviewed by MP3 [32-36].
Survey	Survey drawings need to be prepared.

4.2 IMPACT ON UTILITIES AND SERVICES

Raw water:	No impact
Demineralized water:	Water pipes (water circuit already existing in RR73 and RR77, but not near the PC). Therefore, pipes should be added to cool each rack providing at least 4 l/min.
Compressed air:	TE-VSC: New sector valves feeding require compressed air cabling.
Electricity, cable pulling (power, signal, optical fibres…):	3P+N 20 Arms from ERD with a terminal (model Schneider A9N15658) and 3P+N 2 Arms from EOD with a terminal (model Schneider A9N15656). DC cabling (2x50 mm^2 per polarity) for connection of trim power supplies (WP17)
DEC/DIC:	TE-MPE: DICs reference RQF0908671 (instrumentation), RQF0888406 (PIC), and RFQ0981328 (powering) TE-VSC: DICs (reference RQF0912887 already requested and approved) TE-EPC: RQF0809614 (WorldFIP from trim power converters)
Racks (name and location):	The racks to be installed, displaced and removed are listed in Table 4-7.
Vacuum (bake outs, sectorisation…):	All changes of the vacuum layout are defined in [13, 21]. New beam screen have to furnish the 11 T magnets beam vacuum lines and the non-collimated line in the LEN cryostat. 11 T assessment when performing bake-out on adjacent vacuum equipment (case under discussion – the outcome of this study will be presented in the WP11 interface working group).
Special transport/ handling:	The equipment listed in Tables 4, 5, and 6 needs to be transported and handled in the tunnel and on ground
Temporary storage of conventional/radioactive components:	The de-installed equipment (Table 7) may be radioactive and has to be stored. In particular the two main bending magnets: MB.A9L7 and MB.A9R7
Alignment and positioning:	Marking of the beam points and new jacks heads projections on the ground floor, aligning the jacks’ heads at their nominal position, initial alignment of the components, then plus smoothing (cold temperature) w.r.t. adjacent components. Marking the new slot and alignment after installation.
Scaffolding:	No impact
Controls:	The modification for the controls of QDS (section 2.7.4), nQPS (section 2.8.4) and of the trim power converters (section 2.7.3) are described in the respective sections. New temperature sensors and flow meters will be added [30]. Software updates to SCADA systems for QPS, LHC circuit, PIC, Cryogenics and Survey and vacuum equipment (new gauges and valves) to be foreseen. TE-VSC: New gauges and valves to be integrated in addition to SCADA in VAC LDB. The configuration and settings of the high level LSA controls must be adapted to include the new trim converter of the 11 T dipole. The trim converter must also be included in the PC interlock server configuration which ensures that the PC operates at the correct current during all LHC beam phases.
GSM/WIFI networks:	GSM should be available during the activity as communication means complementary to the red phones in case of emergency.
Cryogenics:	The impact on cryogenics is described in detail in Section 2.4.

Contractor(s):	No
Surface building(s):	No impact
Others:	The N-line as well as the contained superconducting busbars are around 8 cm too short due to the required deviation in the TCLD section. The extension of the line N will follow a similar principle as the one approved for the replacement of a cryodipole in a dispersion suppressor area, namely B10R1, during LS2 [38]. The SIT team of DISMAC will perform the required work in the tunnel.

5. IMPACT ON COST, SCHEDULE AND PERFORMANCE

5.1 IMPACT ON COST

Detailed breakdown of the change cost:	The total cost of the deliverables of WP11 required for the change described in this ECR is borne by the HL-LHC project.		
Budget code:	**BC**	**Unit**	**Description**
	92515	TE-MSC-SCD	HL-LHC-WP11 Cable (Personnel)
	92516	TE-MSC-MDT	HL-LHC-WP11 Model (Personnel)
	92517	TE-MSC-LMF	HL-LHC-WP11 Series (Personnel) [to be used for transport in the tunnel of the WP11 deliverables to be installed around P7] – The transport of the 11T from the top of the pit to the position and installation on its jacks is to be covered by WP15 BC91278 for installation and 91275 for de-installation
	92518	TE-MSC-CMI	HL-LHC-WP11 Cryostat (Personnel)
	92519	TE-MSC-MM	HL-LHC-WP11 Mag. Meas. (Personnel)
	92520	TE-MSC-TF	HL-LHC-WP11 Cold Test (Personnel)
	92529	TE-MSC-LMF	HL-LHC WP11 Tooling (Personnel)
	92608	TE-MSC-LMF	HL-LHC WP11 Series (Personnel) - CONS
	92582	TE-MSC-LMF	HL-LHC WP11 Components (Personnel)
	92570	TE-MSC-SCD	HL-LHC-WP11 Cable
	92571	TE-MSC-MDT	HL-LHC-WP11 Model
	92572	TE-MSC-LMF	HL-LHC-WP11 Series
	92573	TE-MSC-CMI	HL-LHC-WP11 Cryostat
	92609	TE-MSC-CMI	HL-LHC WP11 Cryostat (Personnel) - CONS
	92574	TE-MSC-MM	HL-LHC-WP11 Mag. Meas.
	92575	TE-MSC-TF	HL-LHC-WP11 Cold Test
	92576	TE-MSC-LMF	HL-LHC WP11 Tooling LMF
	92580	TE-MSC-LMF	HL-LHC WP11-11 T-Series-Spares
	92605	TE-MSC-LMF	HL-LHC WP11-11 T-Tooling LMF (CONS)
	92753	TE-EPC-MPC	HL-LHC WP06B-4 Quadrant Converters
	92580	TE-MSC-LMF	WP11 spare magnets (components)

5.2 IMPACT ON SCHEDULE

Proposed installation schedule:	The magnets will be ready for installation on: First full assembly: 17th of December 2019

	Second full assembly: 14th of April 2020 The detailed installation schedule is kept up-to-date by EN-ACE: https://lhc-coordination.web.cern.ch/content/planning-and-shared-documents
Proposed test schedule (if applicable):	The full test of the deliverables will be performed on surface before the installation starts. The quality control (QC) in the tunnel is included in the schedule. The ELQA tests are part of the machine commissioning.
Estimated duration:	Not applicable
Urgency:	Not applicable
Flexibility of scheduling:	The planning and the flexibility of the schedule will be reviewed by an internal review in July 2019.

5.3 IMPACT ON PERFORMANCE

Mechanical aperture:	No harmful impact on beam aperture is expected by the installation of the 11 T dipoles (see Section 3.2), although the magnet is straight and its mechanical aperture is the same as that of the MBs.
Impedance:	Measurements and simulations suggest no issue with impedance, after the installation of the 11 T dipoles and the TCLD. In detail, an impedance analysis of the system TCLD plus RF-beam screen in the 11 T dipoles showed that electromagnetic modes resonate at about 3 GHz at the extremities of the 11 T dipole RF-screen. As these frequencies are large compared to the beam frequency spectrum, no coupling is expected. These results were confirmed by wakefield and eigenmode simulations. Therefore, the current design of the RF beam screen, as far as WP11 is concerned, is fine from an impedance point of view. Regarding the TCLD collimator, the data obtained by measurements and simulations shows a qualitative match up to 1.5 GHz. In particular, low frequencies (less than 500 MHz), which are most critical for beam dynamics, have been studied in detail and all dominant resonant modes could be identified and are considered none critical for beam dynamics. Discrepancies between measurements and simulations are present for frequencies above 1.5 GHz. However, as the shunt impedance is very low for such high frequencies no impact on beam dynamics is expected.
Optics/MAD-X	No negative impact on beam dynamics is expected. The LHC reference MAD-X file needs to be updated, which will be done only after the LHC layout database will contain the needed information. The exact positioning of the magnets has been agreed on.
Electron cloud (NEG coating, solenoid…)	The stronger magnetic field has an impact on the emission of synchrotron radiation from the beam. In particular it results in an increase of the radiated power and in a shift of the critical energy of the emitted photon spectrum. This in turn increases the number of electrons "photo-emitted" by the chamber walls. Calculations have been performed showing that this increase is very limited, and that no visible effect is expected on the heat load on the cryogenics and on the e-cloud build-up.
Vacuum performance:	No impact on vacuum, cryogenic beam vacuum. The impact of the fringe field from the 11 T dipole in the same order as for the MBs (around 10 mT). Therefore, no impact on the vacuum equipment is expected.
Machine protection	Flux-jumps in the long magnets require adapting the settings of the quench protection system below 6 kA. The detailed values are summarized in the HL-LHC ECR, Positioning of the Quench Heaters on the 11T magnet, LHC-MBH-EC-0004 [38].

	The 11 T dipole circuit-powering and protection is described in [30]. The impact of the installation of the 11 T dipole on the nominal operation and on failure scenarios in the RB circuits and the TRIM circuit was studied. The results are described in detail in [40].
Cryogenics	No impact.
Others:	The impact of the magnetic forces due to the fringe field between the cold mass and the ferromagnetic cryostat was studied. For nominal field the horizontal and vertical force is (F_x, F_y) = (0, 3.5) kN. Note that in case only one aperture is powered (F_x, F_y) = (-3.9, 9.9) kN. F_x of the cold mass is pointing in the direction from the powered to the non-powered aperture. If F_y has a negative sign, the force on the cold mass points in the same direction as gravity. The axial forces have not been studied. The amplitude and direction of the forces are considered none critical, as also evident from the tests on the single aperture hybrid magnet. The impact of flux jumps on trim power converter precision performance and field stability at low currents is negligible and discussed in [41].

6. IMPACT ON OPERATIONAL SAFETY

6.1 ÉLÉMENT(S) IMPORTANT(S) DE SECURITÉ

Requirement	Yes	No	Comments
EIS-Access		X	
EIS-Beam		X	
EIS-Machine		X	

6.2 OTHER OPERATIONAL SAFETY ASPECTS

Have new hazards been created or changed?	The 11 T dipole magnet is a pressurized equipment. The 11 T cold mass will be filled with liquid helium. A break of cold-mass helium towards the cryostats' insulation vacuum space has been identified as a risk, with a MCI mass flow of 30 kg/s at 90 K [14]. A copper cold line in the bypass cryostat will be added (pressurized equipment at 1.3bar nominal design pressure). Interconnection of the trim power converter to the RB circuit and a specific procedure of electrical condemnation should be defined for RB.A67, RB.A78, RTA9.L7 and RTA9.R7 circuits to condemn the electrically connected power converters.
Could the change affect existing risk control measures?	The hazard is of the same kind and of the same order of magnitude as for the currently installed device.
What risk controls have to be put in place?	To mitigate the risk of overpressure, safety relief devices are installed. For a DS hydraulic section of 214 m length, and according to the risk assessment cited (break of cold-mass helium) the foreseen number of valves is sufficient. A detailed explanation is provided in Section 3.4. The conformity of the pressurized equipment is being addressed by HSE acting as notified body. HSE will deliver the safety clearance for operation and assess the conformity to the European PED.

	The main dipole circuit are in the interlock for powering phase II, the trims will be also connected to the PIC. The cool down permits will be delivered to allow the safe cool-down of the sectors 67 and 78.
Safety documentation to update after the modification	All the safety documentation asked by the notified body will be archived in EDMS: https://edms.cern.ch/project/CERN-0000183369
Define the need for training or information after the change	No change required for the LHC online training course. The teams intervening on the new equipment need to be trained.

7. WORKSITE SAFETY

7.1 ORGANISATION

Requirement	Yes	No	Comments
IMPACT – VIC:	X		TE-MSC (Sandrine Le Naour) needs to trigger the VIC (Visite d'Inspection Commune) and create the IMPACT
Operational radiation protection (surveys, DIMR…):	X		The area will be surveyed by RP and it is expected that the intervention will be performed under ALARA level 1.
Radioactive storage of material:	X		It is expected that the activation level will allow to store the material in a fenced storage area (supervised radiation zone). Therefore, the radioactive material can be stored in building 180.
Radioactive waste:	X		Volume of radioactive waste will be generated by the worksite itself and will be very limited in volume The removed magnets will be kept as spare Vacuum cleaner for radiological area needed
Non-radioactive waste:	X		Very limited
Fire risk/permit (IS41) (welding, grinding…):	X		The fire permits and the fire mitigation procedures will be defined during the VIC
Alarms deactivation/activation (IS37):	X		The alarms deactivation or activation will be defined during the VIC
Others:	X		This task will be subjected to the WPA coordinated by the LHC coordination team in the framework of the LS2 activities

7.2 REGULATORY TESTS

Requirement	Yes	No	Responsible Group	Comments
Pressure/leak tests:	X		HSE TE-VSC	Work is organized by PSO and was delegated to Arnaud Foussat; PED to be followed Complete leak test will be performed on the entire arc during installation phase.
Electrical tests:	X		TE-MPE	Standard procedures will be applied on the 11 T dipoles as part of the main dipole circuit tests of LHC. The electrical design criteria for the HL-LHC 11 T dipole are listed in [34].

				These procedures have to include the disconnection of the trim power converters when ELQA is performed on RB.A67 or RB.A78.
Others:	X		BE-DSO	PIC will be validated during the DSO tests

7.3 PARTICULAR RISKS

Requirement	Yes	No	Comments
Hazardous substances (chemicals, gas, asbestos…):		X	
Work at height:	X		To be determined during the VIC
Confined space working:		X	
Noise:		X	
Cryogenic risks:		X	The sector will be warmed up and emptied before installation
Industrial X-ray (*tirs radio*):		X	No X-ray testing will be performed in the tunnel. Welds will be inspected only optical with a camera
Ionizing radiation risks (radioactive components):	X		All removed equipment and waste will be tracked by TREC
Electrical risks:	X		The trim current leads are connected to the active part of the MB circuit. The trim current lead active part is being accessible from the flange. Therefore, during the ELQA testing campaign a risk of touching a lively part carrying high voltage is present and mitigation measures have to be taken.
Others:			

8. FOLLOW-UP OF ACTIONS BY THE TECHNICAL COORDINATION

Action	Done	Date	Comments
Carry out site activities:			
Carry out tests:			
Update layout drawings:			
Update equipment drawings:			
Update layout database:			
Update naming database:			
Update optics (MADX)			

Update procedures for maintenance and operations			
Update Safety File according to EDMS document 1177755:			
Others:			

9. REFERENCES

[1] Giorgio Apollinari et al., editors, High-Luminosity Large Hadron Collider (HL-LHC), Technical Design Report V. 0.1, CERN-2017-007-M.

[2] R. Bruce, A. Mereghetti, S. Redaelli, Installation in IR7 of Dispersion Suppressor Collimators (TCLD), LHC-TC-EC-0013.

[3] Pascal Dominik Hermes, et al. LHC Heavy-Ion Collimation Quench Test at 6.37Z TeV. CERN-ACC-NOTE-2016-0031, 2016

[4] Cristina Bahamonde Castro et al., Energy deposition from collimation losses in the DS region at P7, Talk at the 8th HL-LHC collaboration meeting, https://indico.cern.ch/event/742082/contributions/3085132/

[5] ColUSM #89 meeting, https://indico.cern.ch/event/646799

[6] ColUSM #94 meeting, https://indico.cern.ch/event/666560

[7] B. Auchmann et al., Testing beam-induced quench levels of LHC superconducting magnets, Phys. Rev. ST Accel. Beams 18, 061002 (2015)

[7] J.M. Jowett et al., Bound-free pair production in LHC Pb-Pb operation at 6.37 Z TeV per beam, in: Proceedings of IPAC2016, Busan, Korea, http://accelconf.web.cern.ch/AccelConf/ipac2016/papers/tupmw028.pdf

[8] E. Skordis, Study of the 2015 top energy LHC collimation quench tests through an advanced simulation chain, in Proceedings of IPAC2017, Copenhagen, Denmark, http://accelconf.web.cern.ch/AccelConf/ipac2017/papers/mopab012.pdf

[9] Luca Bottura et al., Quench performance and assumptions: magnets and cryogenics, Talk at the International Review of the HL-LHC Collimation System, https://indico.cern.ch/event/780182/contributions/3264119/

[10] Rob van Weelderen, WP9 statement on overall heat load, https://indico.cern.ch/event/776391/, 29th of November 2018

[11] HL-LHC crystal collimation day, 19 October 2018, CERN, Geneva, Switzerland, https://indico.cern.ch/event/752062/

[12] Technical coordination committee of HL-LHC, number 62, 29th November 2018, https://indico.cern.ch/event/776391/

[13] Maria Gonzalez de la Aleja (WP15), WP11: 11 T Dipole full assembly integration study, EDMS 1904620.

[14] M. Modena, HL-LHC integration report for installation approval – WP5: TCLD integration study, EDMS 1903950.

[15] Susana Izquierdo Bermudez, Field quality table, https://espace.cern.ch/HiLumi/WP11/_layouts/15/WopiFrame.aspx?sourcedoc=/HiLumi/WP11/Shared%20Documents/field_quality.xlsx&action=default.

[16] Jaime Coello de Portugal et al., Flux jumps effect on emittance, https://indico.cern.ch/event/813823/contributions/3424661/attachments/1843702/3024721/flux_jumps_after_meas.pdf

[17] D. Gamba et al., Impact of flux jumps on orbit stability, https://indico.cern.ch/event/823530/contributions/3443851/attachments/1859522/3055572/OnFluxJumps_v3.pdf

[18] Lucio Fiscarelli et al. (2018). "Field Quality of MBH 11 T Dipoles for HL-LHC and Impact on Beam Dynamic Aperture", IEEE Trans. Appl. Supercond. 28 4004005.

[19] Alignment WG meeting, https://indico.cern.ch/category/9489/

[20] Giuseppe Bregliozzi and Eric Page, "New Vacuum Pumping Ports in the ARCs linked to the 11T and TCLDs Installation", EDMS 1966384 (LHC-V-EC-0015), https://edms.cern.ch/document/1966384/.

[21] Orlando Santos; Eric Page; Pablo Santos Diaz, "Vacuum layout for the installation of TCLD, 11 T & connection cryostat", EDMS 1869428.

[22] Maciej Chorowski et al., "Upgrade on risk analysis following the 080919 incident in the LHC sector 3-4", CERN/ATS/Note/2010/033.

[23] Paul Cruikshank et al., New protection scheme and pressure relief-valve staging of the LHC insulation vacuum enclosure following the 19th September 2008 incident, CERN /ATS/Note/2010/057 (TECH)2010-12-01

[24] Paul Cruikshank et al., Installation of Additional Pressure Relief Devices on the Cryostats of the LHC Arcs and DS, LHC-QJ-EC-0002 (EDMS #1291202).

[25] Rob van Weelderen, Internal Note, Insulation vacuum safety for HiLumi magnet cryostats, EDMS 2110660

[26] Natalia Magdalena Koziol, DN200 valve with two springs, EDMS 2067605

[27] Rob van Weelderen, Functional requirements with respect to cryogenics for HiLumi superconducting magnet cold-masses, EDMS 2110647

[28] Benjamin Bradu, Additional instrumentation for cryogenics beam-induced heat load measurements, LHC-QI-EC-0009, EDMS 2045687.

[29] Davide Gamba et al. "Beam dynamics requirements for HL-LHC electrical circuits. CERN-ACC-2017-0101," CERN, Geneva, 2017.

[30] Alain Antoine et al., "11T dipole Circuit - Powering and protection", Engineering Specification LHC-MBH-ES-0001, EDMS 1764166.

[31] Jeronimo Ortola et al., "Powering Interlock Controller Software Functionality", Functional Specification ATS-CIP-ES-0001 rev 1.0, EDMS 1360776.

[32] Bruno Puccio, Rudiger Schmidt, Markus Zerlauth: "The Hardware Interfaces Between Powering Interlock System, Power Converters And Quench Protection System", Engineering Specification LHC-D-ES-0003 rev 3.0, EDMS No. 368927.

[33] HL-LHC MCF 43, 30 October 2018, https://indico.cern.ch/event/767872/

[34] Daniel Schoerling, HL-LHC-WP11-Interfaces-Meeting-Minutes-°8, https://edms.cern.ch/document/2037121/2

[35] Michele Modena, List of cables to be modified for the Installation of 11T magnets in LHC during LS2, EDMS 1904830.

[36] A-P. Bernardes et al., Activity Technical Coordination during LS2, Role description, ACC-PM-MG-0002, EDMS 2020003

[37] T Catalao da Rosa, Fernandez Menendez Camara, Felix Rodríguez Mateos, "Electircal design criteria for the HL-LHC 11 T dipole", EDMS 1995595.

[38] D. Schoerling and F. Savary, HL-LHC ECR, Positioning of the Quench Heaters on the 11T magnet, EDMS 2134883, LHC-MBH-EC-0004

[39] S. le Naour and J.P. Tock, Integration of an Additional line N Connection Box in a LHC DS Interconnection, EDMS 2134729

[40] M. Maciejewski et al., Integrated Numerical Analysis of the Modified RB Circuit with the 11 T Cryo-Assembly, EDMS 2157321

[41] M. Martino, P. Arpaia, S. Ierardi, Impact of flux jumps on high-precesion powering of Nb3Sn superconducting magnets, IPAC2019, https://ipac2019.vrws.de/papers/tupmp040.pdf